



Published in final edited form as:

Nat Commun. 2014 ; 5: 3337. doi:10.1038/ncomms4337.

Temporal identity transition from Purkinje cell progenitors to GABAergic interneuron progenitors in the cerebellum

Yusuke Seto^{1,2}, Tomoya Nakatani³, Norihisa Masuyama¹, Shinichiro Taya¹, Minoru Kumai³, Yasuko Minaki^{3,†}, Akiko Hamaguchi³, Yukiko U. Inoue¹, Takayoshi Inoue¹, Satoshi Miyashita^{1,4}, Tomoyuki Fujiyama¹, Mayumi Yamada¹, Heather Chapman⁵, Kenneth Campbell⁵, Mark A. Magnuson⁶, Christopher V. Wright⁷, Yoshiya Kawaguchi⁸, Kazuhiro Ikenaka^{9,10}, Hirohide Takebayashi^{9,10,11}, Shin'ichi Ishiwata^{2,12}, Yuichi Ono³, and Mikio Hoshino¹

¹Department of Biochemistry and Cellular Biology, National Institute of Neuroscience, NCNP, 4-1-1 Ogawa-Higashi, Kodaira, Tokyo 187-8502, Japan

²Department of Physics, Major in Integrative Bioscience and Biomedical Engineering, Faculty of Science and Engineering, Waseda University, 3-4-1 Okubo, Shinjuku-ku, Tokyo 169-8555, Japan

³KAN Research Institute Inc., 3F, Kobe MI R&D Center, 6-7-3 Minatojima-minamimachi, Chuo-ku, Kobe 650-0047, Japan

⁴Department of Electrical Engineering and Bioscience, Graduate School of Advanced Science and Engineering, Waseda University, 3-4-1 Okubo, Shinjuku-ku, Tokyo 169-8555, Japan

⁵Division of Developmental Biology, Cincinnati Children's Hospital Medical Center, University of Cincinnati College of Medicine, 3333 Burnet Avenue, Cincinnati, Ohio 45229-3026, USA

⁶Department of Molecular Physiology and Biophysics and Center for Stem Cell Biology, Vanderbilt University School of Medicine, 2213 Garland Avenue, 9465 MRB IV, Nashville, Tennessee 37232-0494, USA

⁷Vanderbilt University Program in Developmental Biology, Department of Cell and Developmental Biology, Vanderbilt University Medical Center, 2213 Garland Avenue, 9465 MRB IV, Nashville, Tennessee 37232-0494, USA

⁸Department of Clinical Application, Center for iPS Cell Research and Application, Kyoto University, 53 Kawahara-cho, Shogoin, Sakyo-ku, Kyoto 606-8507, Japan

Correspondence and requests for materials should be addressed to Y.O. (y-ono@kan.eisai.co.jp) or to M.H. (hoshino@ncnp.go.jp).

[†]Present address: Center for iPS Cell Research and Application, Kyoto university, 53 Kawahara-cho, shogoin, Sakyo-ku, Kyoto 606-8507, Japan.

Author contributions

Y.S. designed and performed the experiments, analysed the data and wrote the manuscript. T.N. and Y.M. helped with analyses on *pN3-Gsx1* Tg, *Olig1/2* dKO and *Gsx1* KO lines. N.M. helped with construction of *Olig2* expression vector and *in utero* electroporation. S.T. generated anti-Ptf1a. M.K. generated *pN3-Gsx1* Tg, *Olig2* KO, *Olig1/2* dKO lines. A.H. generated *Olig1/2* dKO ES cell. Y.U.I. and T.I. also helped with generating *pN3-Gsx1* Tg line. S.M. and T.F. helped with immunohistochemistry. M.Y. also helped with immunohistochemistry and *in utero* electroporation. H.C. and K.C. helped with the analysis on *Gsx1* function. M.A.M. made *Ptf1a-YFP* knock-in line. Y.K. and C.V.W. made *Ptf1a-Cre* knock-in line. K.I. and H.T. helped with the analysis on *Olig2* function. S.I. encouraged this work. Y.O. and M.H. designed the experiment, analysed the data and wrote the manuscript.

⁹Division of Neurobiology and Bioinformatics, National Institute for Physiological Sciences, 5-1 Higashiyama, Myodaiji, Okazaki, Aichi 444-8787, Japan

¹⁰Department of Physiological Sciences, School of Life Sciences, Graduate University for Advanced Studies, Shonan Village, Hayama, Kanagawa 240-0193, Japan

¹¹Division of Neurobiology and Anatomy, Graduate School of Medical and Dental Sciences, Niigata University, 1-757 Asahimachi, Chuo-ku, Niigata 951-8510, Japan

¹²Waseda Bioscience Research Institute in Singapore, Waseda University, 11 Biopolis Way, #05-01/02, Helios, Singapore 138667, Republic of Singapore

Abstract

In the cerebellum, all GABAergic neurons are generated from the Ptf1a-expressing ventricular zone (Ptf1a domain). However, the machinery to produce different types of GABAergic neurons remains elusive. Here we show temporal regulation of distinct GABAergic neuron progenitors in the cerebellum. Within the Ptf1a domain at early stages, we find two subpopulations; dorsally and ventrally located progenitors that express *Olig2* and *Gsx1*, respectively. Lineage tracing reveals the former are exclusively Purkinje cell progenitors (PCPs) and the latter Pax2-positive interneuron progenitors (PIPs). As development proceeds, PCPs gradually become PIPs starting from ventral to dorsal. In gain- and loss-of-function mutants for *Gsx1* and *Olig1/2*, we observe abnormal transitioning from PCPs to PIPs at inappropriate developmental stages. Our findings suggest that the temporal identity transition of cerebellar GABAergic neuron progenitors from PCPs to PIPs is negatively regulated by *Olig2* and positively by *Gsx1*, and contributes to understanding temporal control of neuronal progenitor identities.

The cerebellum represents a good model system to investigate the molecular machinery underlying specification of neuron subtypes, because it comprises several neuronal types that are distinct in terms of their morphological, physiological and immunohistochemical features. During development, the neuroepithelium of the alar plate of rhombomere 1 generates all cerebellar neuron types¹⁻⁴. Cerebellar neuron-producing neuroepithelium can be divided into two regions; the rhombic lip and the ventricular zone (VZ). All types of cerebellar GABAergic neurons are generated from the VZ that expresses the basic helix-loop-helix (bHLH) transcription factor, pancreatic transcription factor 1a (Ptf1a) that is required for GABAergic neuron production⁵. Coincidentally, Machold *et al.*⁶ and Wang *et al.*⁷ reported that cerebellar glutamatergic neurons are derived from the rhombic lip that expresses *Atoh1*, which is indispensable for producing glutamatergic neurons.

Among cerebellar GABAergic neurons, there are several types of neurons that have distinct characteristics. While Purkinje cells are projection neurons that express *Cor12/Skor2* from early developmental stages⁸, all cerebellar interneurons (INs) such as Golgi, stellate, basket cells and INs in the deep cerebellar nuclei (DCN) express *Pax2* (ref. 9). Therefore, we will refer to cerebellar GABAergic interneurons as 'Pax2 + INs' in this report. The mechanisms that specify each GABAergic subtype remains unclear.

Birthdating studies using ³H-thymidine and BrdU¹⁰⁻¹⁵, as well as adenovirus¹⁶ have revealed that each type of neuron is generated at distinct developmental stages. Purkinje

cells appear relatively early (E10.5~13.5 in mice), Golgi cells a little later (E13.5~postnatal day 0) and stellate/basket cells mainly perinatally. In addition, somatic recombination-based clonal analyses suggested that Purkinje, Golgi and basket/stellate cells belong to the same lineage^{17,18}. These data indicate that some temporal information in the Ptf1a-expressing neuroepithelial domain (Ptf1a domain) may be involved in specification of neuronal types. However, the underlying molecular mechanisms have yet to be defined.

Heterochronic transplantation studies have also provided important clues to understanding cerebellar development¹⁹. It has been shown that tissues or dissociated cells taken from cerebellar primordium at early neurogenesis stages can differentiate into all types of cerebellar GABAergic neurons, while those from postnatal cerebellum differentiated only into GABAergic Pax2 + INs^{20,21}. These findings suggested that, while cerebellar primordium at early stages may contain GABAergic neuron progenitors that can give rise to all types of cerebellar GABAergic neurons including Purkinje cells and Pax2 + INs, cerebellar anlage at later stages contain GABAergic neuron progenitors that produce only Pax2 + INs. Although these observations imply that different types of cerebellar GABAergic progenitors have distinct temporal identities, the molecular machinery involved in regulating temporal information remains unclear.

The homeodomain-containing transcription factor, *Gsx1/Gsh1*, is known to be expressed in some brain regions including telencephalon and diencephalon²². Although targeted disruption of the *Gsx1* gene causes pleiotropic abnormalities in pituitary development and results in dwarfism and sexual infantilism²³, its function in other brain regions is not well defined. The bHLH transcription factor, *Olig2*, was first identified as an oligodendrocyte-specific transcription factor and later as an essential factor for specification of motor neurons derived from the pMN domain of the spinal cord²⁴⁻²⁷. Although *Olig2* is also expressed in the VZ of cerebellum²⁸, its function there is unclear.

In this study, we identify two distinct populations of GABAergic neuron progenitors in the Ptf1a domain; dorsally and ventrally located progenitors that express *Olig2* and *Gsx1*, respectively. The former are exclusively Purkinje cell progenitors (PCPs) and the latter Pax2 + IN progenitors (PIPs). As development proceeds, PCPs gradually become PIPs starting from ventral to dorsal. Results from loss-of-as well as gain-of-function experiments suggest the roles for *Olig2* and *Gsx1* in the regulation of the temporal identity transition of GABAergic neuron progenitors from PCPs to PIPs during cerebellar development.

Results

Expression of *Olig2* and *Gsx1* in the Ptf1a domain

Previously, Chizhikov *et al.*²⁹ defined four cellular populations (denoted c1–c4 domains) in the cerebellar primordium via the expression of a few transcription factors. They showed that all cerebellar GABAergic neurons express transcription factors *Lhx1* and *Lhx5* (*Lhx1/5*), which constitute the c2 domain located just above the Ptf1a domain, which is consistent with the finding that all cerebellar GABAergic neurons emerge from the Ptf1a domain⁵. Furthermore, at the early neurogenesis stages (for example, embryonic day (E) 12.5 in mice), we previously subdivided the c2 domain into dorsally (c2d) and ventrally

(c2v) located subdomains that express *Corl2* and *Pax2*, respectively⁸. This raised the possibility that Purkinje cells and *Pax2* + INs are produced from distinct progenitor regions within the *Ptf1a* domain. Therefore, we looked for transcription factors that are expressed differentially along the dorsoventral axis within the *Ptf1a* domain. We found that *Gsx1* and *Olig2* are exclusively expressed in cells of the ventral and dorsal parts of the *Ptf1a* domain at E12.5, respectively (Fig. 1a–d). Even in the boundary region, we could not detect any cells that expressed both transcription factors simultaneously (Fig. 1e–g).

Progenitors for Purkinje cells and *Pax2* + INs

At E12.5, the *Olig2* + region is much larger than that with *Gsx1* + cells (Fig. 1a–d). *Olig2* expression was also observed in the pial side of the cerebellum (arrow in Fig. 1d), but that will not be discussed here. At E12.5, Purkinje cells were found just above the *Olig2* + cells (Supplementary Fig. 1a), while *Pax2* + INs were localized above the *Gsx1* + cells (Supplementary Fig. 1b). These findings suggest that Purkinje cells and *Pax2* + INs arise from the *Olig2* + and *Gsx1* + cells in the *Ptf1a* domain. Next, we performed short-term lineage trace analyses using *Olig2*^{GFP/+} and *Gsx1*^{GFP/+} mice (Supplementary Fig. 2). Because the half-life of GFP is relatively longer than the transcription factors³⁰, we can label cells derived from *Olig2* + and *Gsx1* + cells using GFP expressed under the control of endogenous *Olig2* and *Gsx1* promoters, respectively. In the E12.5 cerebella of *Olig2*^{GFP/+} embryos, GFP-labelled cells derived from the *Olig2* + cells expressed *Corl2* but not *Pax2* (Fig. 2a–d, i–l). This indicates the *Olig2* + cells are PCPs but not PIPs. In contrast, in the E12.5 cerebella of *Gsx1*^{GFP/+} embryos, GFP-labelled cells were immunoreactive to *Pax2* but not *Corl2*, indicating that the *Gsx1* + cells are PIPs (Fig. 2e–h, m–p). These findings indicate that there are two kinds of GABAergic neuron progenitors within the *Ptf1a* domain of the cerebellar primordia: *Olig2* + PCPs and *Gsx1* + PIPs.

Next, we examined the dynamic change of the distribution patterns of *Olig2* + and *Gsx1* + progenitors at different developmental stages. As development proceeds, the region with *Olig2* + progenitors gradually diminishes and disappears by E14.5. Conversely, the region with *Gsx1* + progenitors expands to cover the entire *Ptf1a* domain by E14.5 (Fig. 3a–d). Coincidentally, we observed that *Pax2* + INs reside only in the ventral side of the cerebellum at earlier stages, and their localization expands towards the dorsal side of the cerebellum as development proceeds (Supplementary Fig. 3a–c). This also supports previous findings that Purkinje cells are produced until E13.5 but not at later stages^{16,31,32}. To further examine the expression dynamics across the cerebellum, multiple coronal sections along the anteroposterior axis at different developmental stages were immunostained with *Olig2* and *Gsx1* together with *Ptf1a* (Supplementary Fig. 3d). Although the proportion of *Olig2*- and *Gsx1*-expressing areas differ along the anteroposterior axis, the regions with *Olig2* + progenitors were gradually superseded by those with *Gsx1* + progenitors throughout the cerebellum during development.

One possible explanation for this dynamic change is that, during development, PCPs decrease in number by reduction of the proliferation rate and/or cell death and PIPs increase by enhancement of the proliferation capacity. However, we never detected any apoptotic cells with active caspase 3 in either *Olig2* + or *Gsx1* + progenitors at E12.5 (Supplementary

Fig. 4a–d). In addition, we observed no differences in proliferation capacity between *Olig2* + and *Gsx1* + progenitors at E12.5, as estimated by phosphohistone H3 immunoreactivity (Supplementary Fig. 4e,f) and BrdU incorporation rates (Supplementary Fig. 4g,h). Therefore, this explanation is not likely.

Another explanation for the dynamic change is that PCPs at early neurogenesis stages change their character to become PIPs at later stages. To test this, we performed an ‘Intermediate-term’ lineage trace analysis by using *Olig2^{GFP+}* embryos. As mentioned above, GFP remains detectable in *Olig2*-lineage cells for several days, even after the promoter activity of *Olig2* gene is downregulated. Therefore, if PCPs at earlier stages give rise to PIPs at later stages, some GFP-labelled cells that lose *Olig2* expression might become *Gsx1* + cells or *Pax2* + INs in *Olig2^{GFP+}* embryos at later stages. In fact, some GFP-positive cells were found to express *Gsx1* at E13.5 (Fig. 3e,f) or *Pax2* at E14.5 (Fig. 3g) in *Olig2^{GFP+}* cerebellar primordium. Although we could detect many GFP-labelled cells in *Pax2*-expressing area where postmitotic neurons resided, the number of GFP-labelled cells in the *Gsx1*-expressing area containing mitotic GABAergic progenitors was not very large. We suspect that residual GFP tended to be diluted by cell division in those mitotic progenitors, or degradation of GFP may occur faster in those cells than in postmitotic neurons. Either way, these results indicate that PCPs change their identity to become PIPs at later stages (Fig. 3h). This ‘temporal identity transition from PCPs to PIPs’ seems to gradually take place in a ventral to dorsal direction during development (Fig. 3d).

It is difficult to determine precisely whether *Gsx1* is expressed within the *Ptf1a* domain at the exact time when *Ptf1a* starts to be expressed in the cerebellar primordia. However, we did observe that *Gsx1* is expressed by a very small population of cells in the ventralmost *Ptf1a* domain as early as E11.0 and E11.5 (Supplementary Fig. 5). This suggests that, even at the earliest stage of cerebellar GABAergic neuron production, there exist two populations of GABAergic progenitors, PIPs and PCPs, although the number of PIPs is relatively small. PCPs that occupy most of the *Ptf1a* domain at the earliest stage gradually change their identity to become PIPs at later stages and as a consequence, the *Ptf1a* domain becomes occupied with PIPs by E14.5. In the rest of the manuscript, we will focus particularly on the temporal identity transition of PCPs to PIPs, although we will also assess the earliest population of PIPs in the Discussion.

Investigation of the *Gsx1* function *in vivo*

In order to investigate the function of *Gsx1* in the temporal identity transition, we generated a mouse line (*pN3-Gsx1* Tg) carrying a transgene that was designed to express *Gsx1* under the control of the *Neph3* promoter³³. Because the *Neph3* promoter is a direct target of *Ptf1a*, *Gsx1* should be heterochronically expressed in the entire *Ptf1a* domain even at earlier stages such as E12.5 (ref. 34). Here, we equally divide the *Ptf1a* and *Lhx1/5* + (c2) domains into three regions along the dorsoventral axis for the sake of convenience: ventral, intermediate and dorsal regions (green, yellow and red lines in Figs 1a–d, 4a–h and 5a,e,i,m).

In these transgenic mice, *Gsx1* is expressed by progenitors in the intermediate and dorsal regions of the *Ptf1a* domain in addition to those in the ventral region at E12.5 (Fig. 4a–d). Interestingly, *Olig2* expression in the VZ completely disappears in *pN3-Gsx1* Tg mice (Fig.

4c), indicating that *Gsx1* can suppress the expression of *Olig2*. Next, we examined the effect of induced *Gsx1* expression on the differentiation of Pax2 + INs and Purkinje cells. In E12.5 wild-type cerebella, Pax2 + INs reside only in the ventral region of the Lhx1/5 + area (c2 domain, Fig. 4e). However, in the cerebella of *pN3-Gsx1* Tg mice, the distribution of Pax2 + INs is extended to the end of intermediate region of c2 domain at E12.5 (Fig. 4g). This indicates that, in addition to progenitors in the ventral region, GABAergic neuron progenitors in the intermediate region also acquired identities of PIPs at this stage in these mice. However, only in rare instances could Pax2 + cells be observed in the dorsal region of the c2 domain, suggesting that PIPs do not reside in the dorsal region of the Ptf1a domain even in the transgenic mice. In E12.5 wild-type cerebella, Corl2 + Purkinje cells were found in the intermediate and dorsal regions of c2 domain but less often in the ventral region (Fig. 4f), consistent with the expression pattern of *Olig2* at this stage (Fig. 1d). In the transgenic mice, Purkinje cells are localized in the dorsal region but less often in the intermediate region and rarely in the ventral region, indicating that PCPs reside in the dorsal region but rarely in the ventral and intermediate regions of the Ptf1a domain (Fig. 4h). Together, these findings suggest that PCPs and PIPs reside in the dorsal and intermediate/ventral regions, respectively, in the transgenic mice, while in the wild type, PCPs and PIPs are localized in the dorsal/intermediate and ventral regions of the Ptf1a domain, respectively. To more precisely examine the effect of ectopic *Gsx1* expression on the distribution of PCPs and PIPs, we investigated the fate of cerebellar GABAergic neuron progenitors that had undergone final cell division at E11.5. Intraperitoneal injection of BrdU to pregnant dams at E11.5 was performed, and embryos collected at E12.5, followed by immunostaining (Supplementary Fig. 6a–n). Statistical analyses revealed that PCPs and PIPs at E11.5 were decreased and increased, respectively, in the *pN3-Gsx1* Tg embryos in all cerebellar regions (Supplementary Fig. 6o,p). Interestingly, this phenotype is more severe ventrally.

Similar results were obtained from transient introduction of *Gsx1* into E12.5 cerebella. The *Gsx1* and GFP expression vectors were electroporated into the Ptf1a domain at E12.5 and embryos were fixed at E14.5. Among *Gsx1*-electroporated cells, the ratio of Pax2-expressing cells was increased compared with control (Supplementary Fig. 7b,d,e). In contrast, the ratio of Corl2-positive cells was reduced almost to zero (Supplementary Fig. 7a,c,e). Because the *Gsx1* expression vector contains a strong and ubiquitous promoter³⁵, this strong constitutive expression of *Gsx1* in progenitors as well as progeny neurons may disturb the normal differentiation into Purkinje cells.

Next, we investigated loss-of-function mutants for *Gsx1*. In control cerebella (*Gsx1*^{GFP/+}) at E12.5, cells that were labelled with *Gsx1* promoter-driven GFP never expressed *Olig2* (Fig. 4j,k). However, many GFP-positive cells at the dorsal edge of the GFP-expressing area were found to express *Olig2* in the homozygous cerebella (*Gsx1*^{GFP/GFP}, Fig. 4n,o, arrowheads). This suggests that the cessation of *Olig2* expression in GABAergic neuron progenitors was delayed in the absence of *Gsx1*. Instead, lack of *Gsx1* expression might dorsalize these cells leading to prolonged expression of *Olig2*. Consistently, we also found that Pax2 + INs (Pax2 +, Lhx1/5 +) were greatly reduced in the *Gsx1*^{GFP/GFP} cerebella compared with control heterozygotes (Fig. 4l,m,p,q), suggesting a decrease of PIPs in the mutant at this stage. Statistical data on the number of Pax2 + INs in genetic gain- and loss-of-function

experiments are shown in Fig. 4i. The proposed function of *Gsx1* deduced from the results of these gain- and loss-of-function experiments will be deliberated in the Discussion.

Investigation of the *Olig2* function *in vivo*

Next we tried to determine the function of *Olig2* that is specific for PCPs. First, we examined the phenotype of *Olig2* single knockout (KO) mice, but could not detect any abnormalities in the cerebellar primordia except for ectopic expression of *Olig1*. In the cerebellum of *Olig2* KO embryos, *Olig1*, which was very slightly expressed in the wild-type cerebellum, was upregulated (Supplementary Fig. 8a–c). This brought up the possibility that enhanced expression of *Olig1* may compensate for *Olig2* function in the *Olig2* KO mice. Previous reports have indicated that *Olig1* could compensate for *Olig2* function, at least in some brain regions including midbrain and hindbrain³⁶. We therefore investigated the phenotype of *Olig1/2* double-KO (dKO) mice (Supplementary Fig. 8d).

In the E13.5 cerebella of the *Olig1/2* dKO mice, we still observed *Corl2* + cells (Fig. 5a,e). This suggests that *Olig2* (and *Olig1*) are not indispensable for the generation of Purkinje cells. However, the number of Purkinje cells was reduced especially at the ventral and intermediate regions in the dKO cerebellum (Fig. 5a–h). Conversely, *Pax2* + cells were increased in number, especially at the ventral and intermediate regions (Fig. 5i–p). This eventually results in disorganization of the overall structure of the cerebellum as well as Purkinje cell layer at E18.5 in the double mutants (Supplementary Fig. 8e–j).

To further examine the distribution of PCPs and PIPs in the wild-type and *Olig1/2* dKO cerebella at E12.5, we tried to investigate the fate of the cerebellar GABAergic neuron progenitors that had undergone the final cell division at E12.5. Intraperitoneal injection of BrdU to pregnant dams at E12.5 was performed, and embryos collected at E13.5, followed by immunostaining (Fig. 6a–c). The distribution and number of BrdU-labelled Purkinje cells and *Pax2* + INs were compared between *Olig1/2* dKO embryos and control littermates (Fig. 6d,e). The ratios of BrdU-labelled *Pax2* + INs and BrdU-labelled *Corl2* + Purkinje cells to BrdU-labelled *Lhx1/5* + cells significantly increased and decreased in *Olig1/2* dKO embryos, respectively (Fig. 6f). The distribution of BrdU-labelled *Pax2* + INs was expanded more dorsally in *Olig1/2* dKO embryos. These results indicate that some PCPs in the ventral and intermediate regions are converted to PIPs at E12.5 in the absence of *Olig1/2* expression. Indeed, we observed that the ventral portion of cells expressing *Olig2* promoter-driven GFP became *Pax2* + INs in *Olig1/2* dKO embryos at E12.5 (Fig. 6h), which was never observed in the heterozygous mice (Fig. 6g).

We further investigated the distribution of PCPs and PIPs at other developmental stages (E11.5 or E13.5), by performing basically identical experiments where BrdU was administered at E11.5 or E13.5 and embryos were analysed one day later (Supplementary Fig. 9a–d). Compared with embryos treated with BrdU at E12.5, similar trends were observed in E11.5 and E13.5 BrdU-administered embryos. The ratios of BrdU-labelled *Pax2* + INs and BrdU-labelled *Corl2* + Purkinje cells to BrdU-labelled *Lhx1/5* + cells significantly increased and decreased in *Olig1/2* dKO embryos, respectively, regardless of the date of BrdU administration (Supplementary Fig. 9e,f). On the other hand, the production of total cerebellar GABAergic neurons was similar regardless of the date of

BrdU incorporation (Supplementary Fig. 9g). These findings demonstrate that the decrease and increase of PCPs and PIPs, respectively, during cerebellar development was accelerated in the *Olig1/2* dKO mice and therefore suggest that temporal identity transition from PCPs to PIPs was accelerated in the mutants. Overall, these results lead to the notion that *Olig2* may act as a brake for temporal identity transition (Fig. 7i).

Interestingly, *pN3-Gsx1* Tg and *Olig1/2* dKO embryos exhibit similar phenotypes; decrease and increase of PCPs to PIPs, respectively. We compared the total number of *Corl2*- or *Pax2*-expressing cells between the E12.5 cerebella of *pN3-Gsx1* Tg and *Olig1/2* dKO embryos that were administered with BrdU at E11.5. Statistical analysis clearly showed that the phenotype is much more severe in *pN3-Gsx1* Tg embryos than *Olig1/2* dKO mice (Supplementary Fig. 9h).

Next, we examined whether ectopic expression of *Olig2* in PIPs suppresses the expression of *Gsx1*. *Olig2* expression vector was co-electroporated with the GFP expression vector into the ventral region of the *Ptf1a* domain at E12.5, and brains were harvested at E13.5 (Fig. 7a). We found that ectopically expressed *Olig2* could not suppress the expression of *Gsx1* in the ventral region (Fig. 7b), although *Gsx1* can suppress the expression of *Olig2* when ectopically expressed (Fig. 4a–d).

In those cells electroporated with the *Olig2* vector, both *Olig2* and *Gsx1* were expressed simultaneously (Fig. 7b). We examined the types of neurons that were generated from progenitors expressing both transcription factors. Two days after the electroporation at E12.5, brains were collected for immunostaining (Fig. 7a). In the control brains, some of electroporated cells expressed the interneuron marker *Pax2* (Fig. 7c,g). However, when co-electroporated with the *Olig2* expression vector, *Pax2* expression was rarely observed (Fig. 7e,g). On the other hand, the expression of *Lhx1/5*, a marker for all cerebellar GABAergic neurons, was similar between control and *Olig2*-overexpressed brains (Fig. 7d,f,h). These results indicate that forced expression of *Olig2* in PIPs inhibits proper differentiation to *Pax2* + INs. Previous studies showed that high expression of *Olig2* blocks neuronal maturation³⁷, therefore it is likely the strong ectopic promoter-driven *Olig2* expression in this experiment inhibits proper differentiation of *Pax2* + INs.

Genetic interaction of *Olig2*, *Gsx1* and *Ptf1a* expression

Finally, we examined genetic interaction between *Olig2*, *Gsx1* and *Ptf1a*. *Ptf1a* is known as an indispensable transcription factor for GABAergic neuron specification in the cerebellum⁷. The expression of *Olig2* disappeared specifically in the VZ of *Ptf1a* KO embryos, although its expression at the pial side was not affected (Supplementary Fig. 10a–f), suggesting that *Olig2* may be a downstream target of *Ptf1a* in the VZ (Fig. 7i). Next, we utilized another null allele for the *Ptf1a* gene (*Ptf1a*^{YFP}) in which the *Ptf1a* domain is labelled by a *Ptf1a* promoter-driven YFP. In contrast to *Olig2* expression, the expression of *Gsx1* was maintained in the YFP-positive area of *Ptf1a*-null embryos (*Ptf1a*^{YFP/YFP}) (Supplementary Fig. 10g–r), suggesting that there may be another upstream regulator for *Gsx1* (Fig. 7i). In the *Ptf1a*-null cerebella (*Ptf1a*^{YFP/YFP}) at E13.5, we could not detect any GABAergic inhibitory neurons that were labelled with the specific marker, *Lhx1/5* (Supplementary Fig. 10s,t), consistent with previous findings that no GABAergic neurons were produced in the

Ptf1a mutants⁵. Accordingly, in the *Ptf1a*-mutant cerebella (*Ptf1a*^{YFP/YFP}), Pax2 + INs were not observed in the *Ptf1a* lineage, which were labelled with GFP (Supplementary Fig. 10s,t).

Discussion

In this study, we found there are two distinct subpopulations in cerebellar GABAergic neuron progenitors within the *Ptf1a* domain at E12.5; dorsally located Olig2 + and ventrally localized Gsx1 + progenitors. Short-term lineage analyses with GFP-knock-in mice revealed that Olig2 + and Gsx1 + progenitors are PCPs and PIPs, respectively. Furthermore, our intermediate lineage trace analysis using *Olig2*^{GFP/+} mice showed that PCPs at earlier stages change their character to become PIPs at later stages. We termed this change as ‘temporal identity transition’ of cerebellar GABAergic progenitors. Furthermore, it seems that temporal identity transition occurs earlier ventrally and later dorsally, because Gsx1-positive cells first appear in the ventral side and later in the dorsal side of the *Ptf1a* domain at corresponding developmental stages.

However, our data also implied that a small number of cells express Gsx1 at the most ventral region of the *Ptf1a* domain at a very early stage, while many more cells express Olig2 within the *Ptf1a* domain. Because a previous study reported that Pax2 + INs in the DCN can be produced as early as Purkinje cells¹⁴, these ventrally located Gsx1 + cells may be PIPs that produce Pax2 + INs in the DCN. Therefore, one might imagine that there are two distinct spatially defined regions within the *Ptf1a* domain at the onset of GABAergic neuron production; a small number of PIPs at the ventral most region and large number of PCPs in the other regions of the *Ptf1a* domain. As development proceeds, those PCPs gradually change their identity to become PIPs from ventral to dorsal, until the entire *Ptf1a* domain is occupied with PIPs by E14.5. Because we were interested in the temporal identity transition from PCPs to PIPs, we focused on that issue in this study.

Muguruma *et al.*³⁸ previously succeeded in differentiating ES cells into cerebellar GABAergic neurons. During culture after certain induction procedures, Corl2 + cells are first produced and subsequently Pax2 + cells are generated in cells derived from an ES cell clone. Although that experiment did not directly show that ES-derived PCPs and PIPs are in the same lineage, ES cell-derived PCPs likely also change into PIPs during culturing, given our *in vivo* findings in this study. After the initial induction steps, no extrinsic factors appear to be required to elicit the temporal identity change *in vitro*. This suggests that cerebellar GABAergic progenitors have their own internal clocks that carry temporal information to elicit the temporal identity transition at the appropriate time. Because the temporal identity transition from PCPs to PIPs occurs earlier at the ventral side, the internal clocks of cerebellar GABAergic progenitors may be faster in the ventral region and slower in the dorsal region.

We observed that some Purkinje cells were produced in the *Olig1/2* dKO mice, suggesting that Olig2 (and Olig1) might not be indispensable for Purkinje cell generation. However, Purkinje cells and Pax2 + INs were decreased and increased, respectively, especially at the ventral and intermediate regions. Moreover, BrdU incorporation studies at different developmental stages showed that both the decrease and increase of PCPs and PIPs,

respectively, during cerebellar development were accelerated in the mutant mice. These findings suggest that temporal identity transition from PCPs to PIPs was accelerated in the mutants and therefore suggest that *Olig2* (and *Olig1*) may function as a brake for the temporal identity transition as well as the internal clocks of GABAergic neuron progenitors. The milder phenotype at the dorsal side could be explained from the viewpoint of internal clocks as follows. The internal clocks of dorsally located progenitors are set later than those of ventrally or intermediately localized progenitors in the wild-type mice, acceleration of the internal clocks by loss of *Olig2* (and *Olig1*) may not be sufficient to elicit the temporal identity transition in the dorsal region.

In neither *Olig2^{GFP+}* nor *Olig1^{+/-}*; *Olig2^{GFP+}* cerebella at E12.5, did we ever observe Pax2 + INs that were labelled with GFP. This may imply that the temporal identity transition from PCPs to PIPs do not occur prior to the stage that these Pax2 + INs are produced (for example, E11.5). However, in *Olig1/2* dKO cerebella at E12.5, we observed many GFP-labelled Pax2 + INs. This finding also suggests that the temporal identity transition precociously occurs in the dKO mice.

A gain-of-function experiment using BrdU-injected *pN3-Gsx1* Tg mice showed that forced expression of *Gsx1* caused a decrease and increase of PCPs and PIPs, respectively, at an early stage (E11.5). This phenotype was more severe at the ventral/intermediate regions but milder in the dorsal region. Two explanations are possible for this phenotype. One is that *Gsx1* gives ventralizing spatial information to GABAergic neuron progenitors and gain of this function leads to ventralization of the GABAergic progenitors causing their ectopic transition to PIPs. The other explanation is that *Gsx1* may act as an accelerator for the temporal identity transition as well as the internal clocks of GABAergic neuron progenitors and gain of this function results in precocious temporal identity transition from PCPs to PIPs.

We also observed many *Olig2*-expressing cells within the GFP-labelled region in *Gsx1^{GFP/GFP+}* embryonic cerebella, which are never found in control *Gsx1^{GFP+}*. Consistently, the number of Pax2 + INs was remarkably reduced in the homozygous mutants at E12.5. Similar to the results from the *pN3-Gsx1* Tg mice, this phenotype can also be likewise interpreted. *Gsx1* may give ventralizing information to GABAergic progenitors and loss of this function leads to dorsalization of GABAergic progenitors inhibiting their transition to PIPs. Or, *Gsx1* may act as an accelerator for the internal clocks and loss of this function results in delayed temporal identity transition. Actually, it is difficult to discriminate between these two possibilities. However, because *Olig2* and *Gsx1* are expressed in a complementary pattern and because the loss-of-function mutants for the two genes exhibit opposite phenotypes, it is likely that *Olig2* and *Gsx1* have opposing functions. As *Olig2* was revealed to function as a brake for the temporal identity transition, we predict that *Gsx1* may function as an accelerator for it. However, further investigation is required.

This study showed that *Gsx1* suppresses the expression of *Olig2*, but that *Olig2* cannot suppress *Gsx1* expression. This raises a possibility that the accelerating effect on temporal identity transition by *Gsx1* may be accomplished through downregulation of *Olig2* expression, because *Olig2* works as a brake for temporal identity transition. However, we

believe *Gsx1* may not only suppress the expression of *Olig2* but it may work via some additional pathways for the progression of temporal identity transition, because the severity was much greater in *pN3-Gsx1* Tg than in *Olig1/2* dKO mice (Supplementary Fig. 9h). In addition, forced expression of *Olig2* in PIPs using an expression vector with a strong promoter cannot suppress the expression of *Gsx1*. Actually, few cells were observed to express both proteins in the Ptf1a domain. Therefore, the asymmetry in genetic interaction between the expression of *Olig2* and *Gsx1* may enable the unidirectional progression of temporal identity transition from the ventral region to the dorsal region. In addition, we showed that Ptf1a is required for the expression of *Olig2* but not for that of *Gsx1*. The genetic relationship among transcription factors is summarized in Fig. 7i.

In vertebrates and invertebrates, it is likely that neuronal progenitors have two types of identities; spatial and temporal. In fruitflies, one hemineuromere has about 30 neuroblasts, which are localized in spatially distinct locations, express different sets of transcription factors and produce distinct types of neurons and glia^{39,40}. Moreover, each neuroblast changes its temporal identity during development, to generate various neurons/glia types⁴¹. Many studies have been done to investigate the temporal identities of neuroblasts in *Drosophila*, revealing the involvement of transcription factors such as Hunchback, Krüppel, Pdm and Castor in defining the temporal identities of neuroblasts. In addition to such ‘temporal identity determinants’, several ‘temporal identity transition regulators’ like Seven up, Dan/Danr, and so on, which control the speed of progression of temporal identity transition have been identified⁴².

In the mammalian telencephalon, glutamatergic and GABAergic neurons are generated from spatially distinct progenitors; dorsal and ventral neuroepithelia, respectively⁴³. Their spatial identities are thought to be defined by bHLH transcription factors, such as Neurogenin1/2 and achaete-scute complex-like 1 (also called Mash1). In addition, even from the same neuroepithelial regions in the dorsal telencephalon, different types of neurons can be produced; early-born and late-born neurons differentiate into deep-layer and superficial-layer neurons, respectively, with distinct characteristics⁴⁴. This indicates that the temporal identity of glutamatergic progenitors varies as development proceeds. However, the molecular mechanisms controlling the temporal identities in mammals are still elusive.

In the mammalian cerebellar primordium, we and others have previously suggested that two bHLH proteins, Atoh1 and Ptf1a are involved in specifying the spatial identities of neural progenitors^{5–7,45}. In this work, we found two types of GABAergic progenitors, PCPs and PIPs, which are in the same lineage but have distinct temporal identities. Unfortunately, the temporal identity determinants for PCPs and PIPs remain elusive, as the presence of Purkinje cells or Pax2 + INs in either loss of *Olig2* or *Gsx1* gene could still be observed. However, we believe that we have found candidates for the temporal identity transition regulators that negatively and positively control the speed of the temporal identity transition of GABAergic neuron progenitors.

There are thousands of neuron types in the nervous system, each of which has morphologically, electrophysiologically and immunohistochemically distinct characteristics. Although the diversity of neurons may be, at least in part, explained by the diversity of

spatial and temporal identities of neuronal progenitors, the underlying molecular machinery is still elusive, especially regarding the temporal identities in vertebrates. Further studies are required to understand the molecular mechanisms that produce the variety of neuronal types.

Methods

Animals

All animal experiments in this study have been approved by the Animal Care and Use Committee of the National Institute of Neuroscience, Japan. *Ptf1a^{YFP}*, *Ptf1a^{Cre}* lines were described previously^{46–48}. *Olig2^{GFP}* and *Gsx1^{GFP}* lines were generated by replacing the ORF sequence of each gene with GFP cDNA, respectively. *Olig1^{null} Olig2^{GFP}* was generated by deleting the ORF of *Olig1* gene and replacing the ORF sequence of *Olig2* gene with GFP cDNA (see also Supplementary Figs 2,5). *pN3-Gsx1* Tg was generated by a standard method⁴⁹. A quantity of 3.5 ng μl^{-1} of linearized and agarose gel purified plasmid DNA was microinjected into pronuclei of fertilized eggs derived from the superovulated B6C3F1 mouse strain (SLC, Japan). The construct for this line was generated by inserting the ORF sequence of *Gsx1* into a pN3 vector.

Antibodies and immunohistochemistry

Primary antibodies used in this study were anti-BrdU (1:200; rat; ABD Serotec, Kidlington, UK), *Corl2* (1:500; rabbit polyclonal), GFP (1:10; rat; a kind gift from Dr A. Imura, Kyoto University, Kyoto, Japan), *Gsx1* (1:250; rat), *Lhx1/5* (1:3,000; mouse; DSHB, Iowa City, IO, USA), *Olig2* (1:500; goat; R&D Systems, Minneapolis, MN, USA), *Pax2* (1:200; rabbit; Invitrogen, Carlsbad, CA, USA), *Ptf1a* (1:200; rabbit), *RORa* (1:2,000; goat; Santa Cruz Biotechnology, Santa Cruz, CA, USA). Rat monoclonal anti-*Gsx1* mAb was raised against GST-*Gsx1* 1–72 amino acids (aa). Anti-*Ptf1a* antibody was generated as follows. The fragment of mouse *Ptf1a* full length (Full: 1–324 aa) or -amino-terminal (NT: 1–145 aa) was inserted into pMAL-c2 (New England Laboratories, Beverly, MA) or pGEX-4T-2 (Amersham Pharmacia Biotech, Buckinghamshire, UK), respectively. Maltose-binding protein and glutathione *S*-transferase (GST) fusion proteins were expressed in *Escherichia coli* BL21 (DE3) and purified according to the manufacturer's instructions. Polyclonal rabbit anti-*Ptf1a* antibody was prepared against maltose-binding protein-*Ptf1a*-Full as an antigen, and then purified by use of GST-*Ptf1a*-NT. This antibody detected no signals in the *Ptf1a*-null (*Ptf1a^{Cre/Cre}*) mutant. Immunohistochemistry was performed as follows. Embryos were fixed with 4% paraformaldehyde in PBS. After the cryoprotection, embryos were embedded in OCT compound. Cryosections were made in the thickness of 14 μm . Sections were treated with 0.5% BSA in PBS containing 0.2% Triton X-100 (blocking buffer) at room temperature for 1 h and subsequently incubated with antibodies listed below in blocking buffer at 4 °C for 20 h. Specimens were subsequently rinsed with PBS and incubated with the secondary antibody at room temperature for 2 h. Tissues were examined by fluorescent microscopy. Coloured lines that divide VZ or c2 domain (where cerebellar GABAergic neurons reside) into ventral (green), intermediate (yellow) and dorsal (red) in Figs 1,4,5, were drawn by equally dividing the length of the bottom of VZ or c2 domain by three. Dashed lines that divide c2 domain into ventral, intermediate and dorsal area in

Supplementary Fig. 6 were drawn perpendicularly to the tangent of the points, which equally divide the length of the bottom of c2 domain by three.

BrdU incorporation experiment

Pregnant mice (E11.5, E12.5 and E13.5) were given intraperitoneal injections of BrdU at 100 mg kg⁻¹. Twenty-four hours after the BrdU injection, embryos were fixed and subjected to immunohistochemical analyses as follows. After the immunostaining with antibodies besides BrdU, sections were post-fixed with 4% paraformaldehyde in PBS at room temperature for 20 min. After the fixation, sections were treated with 2N hydrochloric acid at 37 °C for 30 min. Then sections were washed and immunostaining with anti-BrdU was performed. The number of BrdU, Lhx1/5-double-positive cells and BrdU, Lhx1/5, Corl2 (or Pax2)-triple-positive cells were quantified. BrdU, Lhx1/5-double-positive cells were counted as neurons generated during the 24 h after the BrdU injection. By calculating the rate of triple-positive cells to double-positive cells and plotting the positions of these cells, we roughly estimated the number and distribution of PCPs and PIPs in the progenitor domain at the injected stages. To analyse the BrdU incorporation rates of PIPs and PCPs in E12.5 wild-type embryos, pregnant mice (E12.5) were given two intraperitoneal injections of BrdU at 50 mg kg⁻¹ with a 30-min interval. One hour after the first BrdU injection, mice were killed and embryonic brains were fixed and subjected to immunohistochemical analyses.

***In utero* electroporation**

One microliter of plasmid DNA (mixture of pCAG-EGFP-N3: 0.5 mg ml⁻¹ and pCAG-Olig2: 1 mg ml⁻¹ or pCAG-Gsx1: 1 mg ml⁻¹) in TE (Tris-EDTA; 10 mM Tris, 1 mM EDTA, pH 7.5) containing Fast Green was injected into the fourth ventricles of embryonic brains from outside the uterus with a glass micropipette (G-1.0; Narishige). Holding the embryo *in utero* with forceps-type electrodes (NEPA GENE), 50 ms of 40 V electronic pulses were delivered five times at intervals of 450 ms with a square electroporator (Nepa Gene). pCAG-Olig2 and pCAG-Gsx1 vector was generated by inserting the ORF sequence into the cloning site of pCAG2-en.

Supplementary Material

Refer to Web version on PubMed Central for supplementary material.

Acknowledgments

We are grateful to Dr T. Imai (KAN Research Institute Inc.) and Dr F. Rossi for constant support and encouragement. We would like to thank Dr David J. Anderson and Dr Ruth Yu for a mouse line and comments, respectively. This work is supported by grants from the MEXT, Naito foundation, Intramural Research Grants (24-12, 25-3) for Neurological and Psychiatric Disorders of NCNP and Health Science Research Grant for Research on Psychiatric and Neurological Diseases and Mental Health (H23-001) from the Japanese Ministry of Health, Labor and Welfare.

References

1. Chizhikov V, Millen KJ. Development and malformations of the cerebellum in mice. *Mol Genet Metab.* 2003; 80:54–65. [PubMed: 14567957]

2. Millet S, Bloch-Gallego E, Simeone A, Alvarado-Mallart RM. The caudal limit of Otx2 gene expression as a marker of the midbrain/hindbrain boundary: a study using *in situ* hybridisation and chick/quail homotopic grafts. *Development*. 1996; 122:3785–3797. [PubMed: 9012500]
3. Wingate RJ, Hatten ME. The role of the rhombic lip in avian cerebellum development. *Development*. 1999; 126:4395–4404. [PubMed: 10498676]
4. Zervas M, Millet S, Ahn S, Joyner AL. Cell behaviors and genetic lineages of the mesencephalon and rhombomere 1. *Neuron*. 2004; 43:345–357. [PubMed: 15294143]
5. Hoshino M, et al. Ptf1a, a bHLH transcriptional gene, defines GABAergic neuronal fates in cerebellum. *Neuron*. 2005; 47:201–213. [PubMed: 16039563]
6. Machold R, Fishell G. Math1 is expressed in temporally discrete pools of cerebellar rhombic-lip neural progenitors. *Neuron*. 2005; 48:17–24. [PubMed: 16202705]
7. Wang VY, Rose MF, Zoghbi HY. Math1 expression redefines the rhombic lip derivatives and reveals novel lineages within the brainstem and cerebellum. *Neuron*. 2005; 48:31–43. [PubMed: 16202707]
8. Minaki Y, Nakatani T, Mizuhara E, Inoue T, Ono Y. Identification of a novel transcriptional corepressor, Corl2, as a cerebellar Purkinje cell-selective marker. *Gene Expr Pat*. 2008; 8:418–423.
9. Maricich SM, Herrup K. Pax-2 expression defines a subset of GABAergic interneurons and their precursors in the developing murine cerebellum. *J Neurobiol*. 1999; 41:281–294. [PubMed: 10512984]
10. Batini C, Compoin C, Buisseret-Delmas C, Daniel H, Guegan M. Cerebellar nuclei and the nucleocortical projections in the rat: retrograde tracing coupled to GABA and glutamate immunohistochemistry. *J Comp Neurol*. 1992; 315:74–84. [PubMed: 1371781]
11. Chan-Palay V, Palay SL, Brown JT, Van Itallie C. Sagittal organization of olivocerebellar and reticulocerebellar projections: autoradiographic studies with 35S-methionine. *Exp Brain Res*. 1977; 30:561–576. [PubMed: 598441]
12. De Zeeuw CI, Berrebi AS. Postsynaptic targets of Purkinje cell terminals in the cerebellar and vestibular nuclei of the rat. *Eur J Neurosci*. 1995; 7:2322–2333. [PubMed: 8563981]
13. Leto K, Carletti B, Williams IM, Magrassi L, Rossi F. Different types of cerebellar GABAergic interneurons originate from a common pool of multipotent progenitor cells. *J Neurosci*. 2006; 26:11682–11694. [PubMed: 17093090]
14. Sudarov A, et al. Ascl1 genetics reveals insights into cerebellum local circuit assembly. *J Neurosci*. 2011; 31:11055–11069. [PubMed: 21795554]
15. Sultan F, Czubyko U, Thier P. Morphological classification of the rat lateral cerebellar nuclear neurons by principal component analysis. *J Comp Neurol*. 2003; 455:139–155. [PubMed: 12454981]
16. Hashimoto M, Mikoshiba K. Mediolateral compartmentalization of the cerebellum is determined on the “birth date” of Purkinje cells. *J Neurosci*. 2003; 23:11342–11351. [PubMed: 14672998]
17. Mathis L, Bonnerot C, Puelles L, Nicolas JF. Retrospective clonal analysis of the cerebellum using genetic lacZ/lacZ mouse mosaics. *Development*. 1997; 124:4089–4104. [PubMed: 9374405]
18. Mathis L, Nicolas JF. Progressive restriction of cell fates in relation to neuroepithelial cell mingling in the mouse cerebellum. *Dev Biol*. 2003; 258:20–31. [PubMed: 12781679]
19. Carletti B, Rossi F. Neurogenesis in the cerebellum. *Neuroscientist*. 2008; 14:91–100. [PubMed: 17911211]
20. Jankovski A, Rossi F, Sotelo C. Neuronal precursors in the postnatal mouse cerebellum are fully committed cells: evidence from heterochronic transplantations. *Eur J Neurosci*. 1996; 8:2308–2319. [PubMed: 8950095]
21. Carletti B, Grimaldi P, Magrassi L, Rossi F. Specification of cerebellar progenitors after heterotopic-heterochronic transplantation to the embryonic CNS *in vivo* and *in vitro*. *J Neurosci*. 2002; 22:7132–7146. [PubMed: 12177209]
22. Valerius MT, et al. Gsh-1: a novel murine homeobox gene expressed in the central nervous system. *Dev Dyn*. 1995; 203:337–351. [PubMed: 8589431]
23. Li H, Zeitler PS, Valerius MT, Small K, Potter SS. Gsh-1, an orphan Hox gene, is required for normal pituitary development. *EMBO J*. 1996; 15:714–724. [PubMed: 8631293]

24. Lu QR, et al. Sonic hedgehog-regulated oligodendrocyte lineage genes encoding bHLH proteins in the mammalian central nervous system. *Neuron*. 2000; 25:317–329. [PubMed: 10719888]
25. Zhou Q, Wang S, Anderson DJ. Identification of a novel family of oligodendrocyte lineage-specific basic helix-loop-helix transcription factors. *Neuron*. 2000; 25:331–343. [PubMed: 10719889]
26. Takebayashi H, et al. The basic helix-loop-helix factor olig2 is essential for the development of motoneuron and oligodendrocyte lineages. *Curr Biol*. 2002; 12:1157–1163. [PubMed: 12121626]
27. Mizuguchi R, et al. Combinatorial roles of Olig2 and Neurogenin2 in the coordinated induction of pan-neuronal and subtype-specific properties of motoneurons. *Neuron*. 2001; 31:757–771. [PubMed: 11567615]
28. Takebayashi H, et al. Non-overlapping expression of Olig3 and Olig2 in the embryonic neural tube. *Mech Dev*. 2002; 113:169–174. [PubMed: 11960707]
29. Chizhikov VV, et al. The roof plate regulates cerebellar cell-type specification and proliferation. *Development*. 2006; 133:2793–2804. [PubMed: 16790481]
30. Shaker T, Dennis D, Kurrasch DM, Schuurmans C. Neurog1 and Neurog2 coordinately regulate development of the olfactory system. *Neural Dev*. 2012; 7:28. [PubMed: 22906231]
31. Miale IL, Sidman RL. An autoradiographic analysis of histogenesis in the mouse cerebellum. *Exp Neurol*. 1961; 4:277–296. [PubMed: 14473282]
32. Wang VY, Zoghbi HY. Genetic regulation of cerebellar development. *Nat Rev Neurosci*. 2001; 2:484–491. [PubMed: 11433373]
33. Mizuhara E, et al. Purkinje cells originate from cerebellar ventricular zone progenitors positive for Neph3 and E-cadherin. *Dev Biol*. 2010; 338:202–214. [PubMed: 20004188]
34. Nishida K, Hoshino M, Kawaguchi Y, Murakami F. Ptf1a directly controls expression of immunoglobulin superfamily molecules Neph3 and Neph3 in the developing central nervous system. *J Biol Chem*. 2009; 285:373–380. [PubMed: 19887377]
35. Niwa H, Yamamura K, Miyazaki J. Efficient selection for high-expression transfectants with a novel eukaryotic vector. *Gene*. 1991; 108:193–199. [PubMed: 1660837]
36. Zhou Q, Anderson DJ. The bHLH transcription factors OLIG2 and OLIG1 couple neuronal and glial subtype specification. *Cell*. 2002; 109:61–73. [PubMed: 11955447]
37. Lee SK, Lee B, Ruiz EC, Pfaff SL. Olig2 and Ngn2 function in opposition to modulate gene expression in motor neuron progenitor cells. *Genes Dev*. 2005; 19:282–294. [PubMed: 15655114]
38. Muguruma K, et al. Ontogeny-recapitulating generation and tissue integration of ES cell-derived Purkinje cells. *Nat Neurosci*. 2010; 13:1171–1180. [PubMed: 20835252]
39. Broadus J, et al. New neuroblast markers and the origin of the aCC/pCC neurons in the *Drosophila* central nervous system. *Mech Dev*. 1995; 53:393–402. [PubMed: 8645605]
40. Doe CQ. Molecular markers for identified neuroblasts and ganglion mother cells in the *Drosophila* central nervous system. *Development*. 1992; 116:855–863. [PubMed: 1295739]
41. Pearson BJ, Doe CQ. Specification of temporal identity in the developing nervous system. *Annu Rev Cell Dev Biol*. 2004; 20:619–647. [PubMed: 15473854]
42. Kohwi M, Hiebert LS, Doe CQ. The pipsqueak-domain proteins Distal antenna and Distal antenna-related restrict Hunchback neuroblast expression and early-born neuronal identity. *Development*. 2011; 138:1727–1735. [PubMed: 21429984]
43. Schuurmans C, Guillemot F. Molecular mechanisms underlying cell fate specification in the developing telencephalon. *Curr Opin Neurobiol*. 2002; 12:26–34. [PubMed: 11861161]
44. Kwan KY, Sestan N, Anton ES. Transcriptional co-regulation of neuronal migration and laminar identity in the neocortex. *Development*. 2012; 139:1535–1546. [PubMed: 22492350]
45. Hoshino M. Molecular machinery governing GABAergic neuron specification in the cerebellum. *Cerebellum*. 2006; 5:193–198. [PubMed: 16997750]
46. Burlison JS, Long Q, Fujitani Y, Wright CV, Magnuson MA. Pdx-1 and Ptf1a concurrently determine fate specification of pancreatic multipotent progenitor cells. *Dev Biol*. 2008; 316:74–86. [PubMed: 18294628]
47. Fujitani Y, et al. Ptf1a determines horizontal and amacrine cell fates during mouse retinal development. *Development*. 2006; 133:4439–4450. [PubMed: 17075007]

48. Kawaguchi Y, et al. The role of the transcriptional regulator Ptf1a in converting intestinal to pancreatic progenitors. *Nat Genet.* 2002; 32:128–134. [PubMed: 12185368]
49. Inoue T, et al. Analysis of mouse *Cdh6* gene regulation by transgenesis of modified bacterial artificial chromosomes. *Dev Biol.* 2008; 315:506–520. [PubMed: 18234175]

Author Manuscript

Author Manuscript

Author Manuscript

Author Manuscript

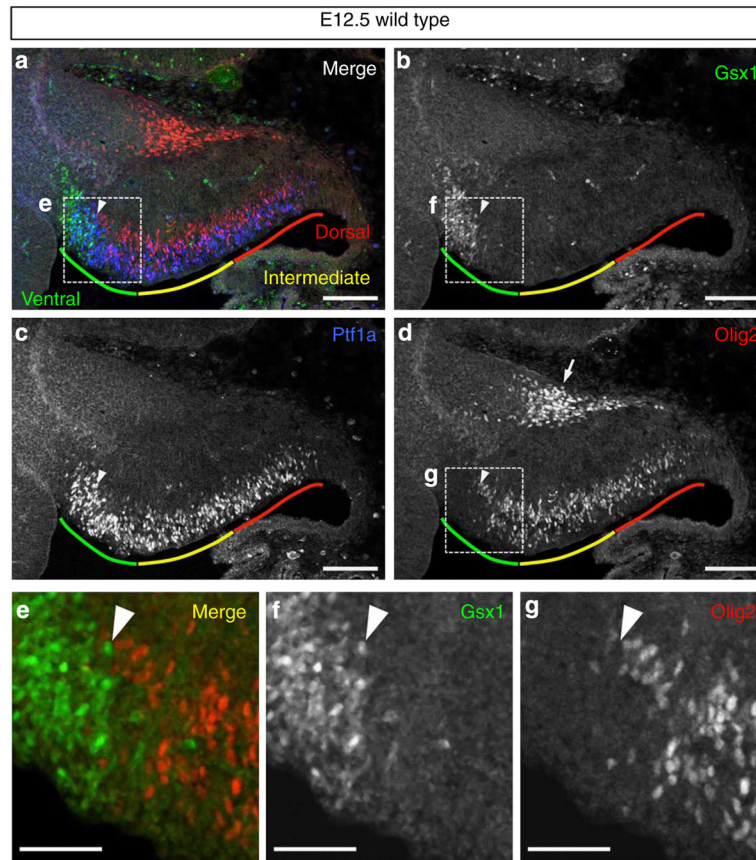


Figure 1. Mutually exclusive expression of Olig2 and Gsx1 in the cerebellar VZ at E12.5
(a–d) Wild-type cerebellar primordium at E12.5 stained with antibodies for Gsx1, Olig2 and Ptf1a. Coloured lines indicate ventral (green), intermediate (yellow) and dorsal (red) regions of cerebellar VZ, respectively. Arrowheads indicate the boundary between Gsx1 and Olig2-expressing progenitors. **(e–g)** Higher-magnification images of the rectangular regions in **(a)**, **(b)** and **(d)**, respectively. Scale bars represent **(a–d)** 100 μm , **(e–g)** 50 μm .

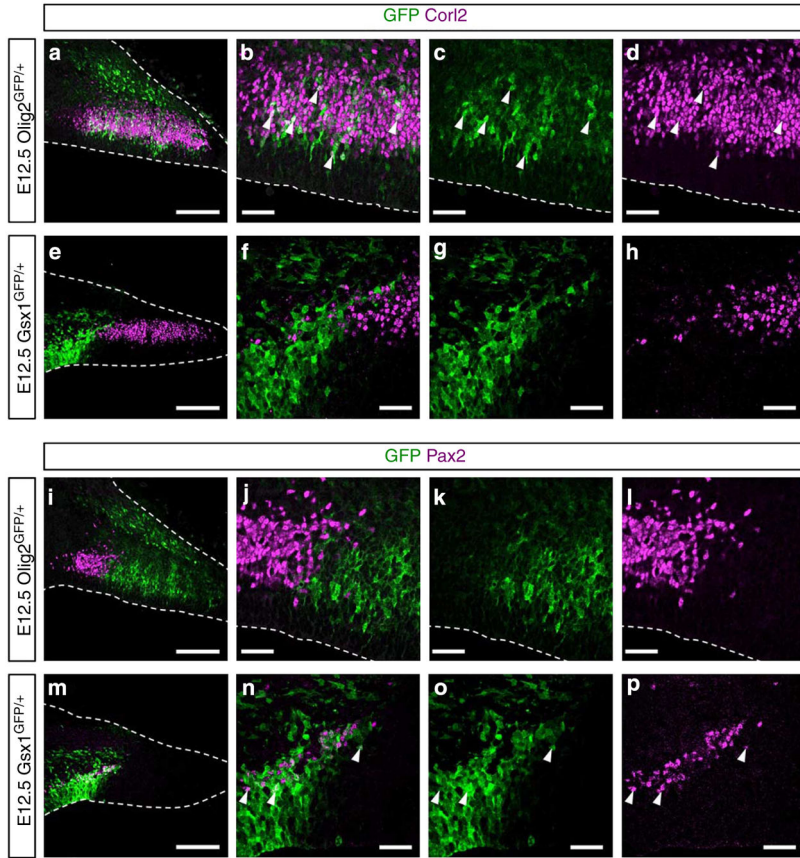


Figure 2. Cerebellar progenitors for Purkinje cells and Pax2 + INs

(a–p) Lineage tracing analyses using *Olig2*^{GFP/+} (a–d,i–l) and *Gsx1*^{GFP/+} (e–h,m–p) embryos. (a–h) In the cerebellum, Purkinje cells are specifically labelled with an antibody for Corl2. (i–p) GABAergic interneurons are labelled with an antibody for Pax2. Arrowheads highlight double-stained cells. Stages, genotypes and antibodies are indicated. Scale bars represent (a,e,i and m) 100 μ m, (b–d,f–h,j–l and n–p) 25 μ m.

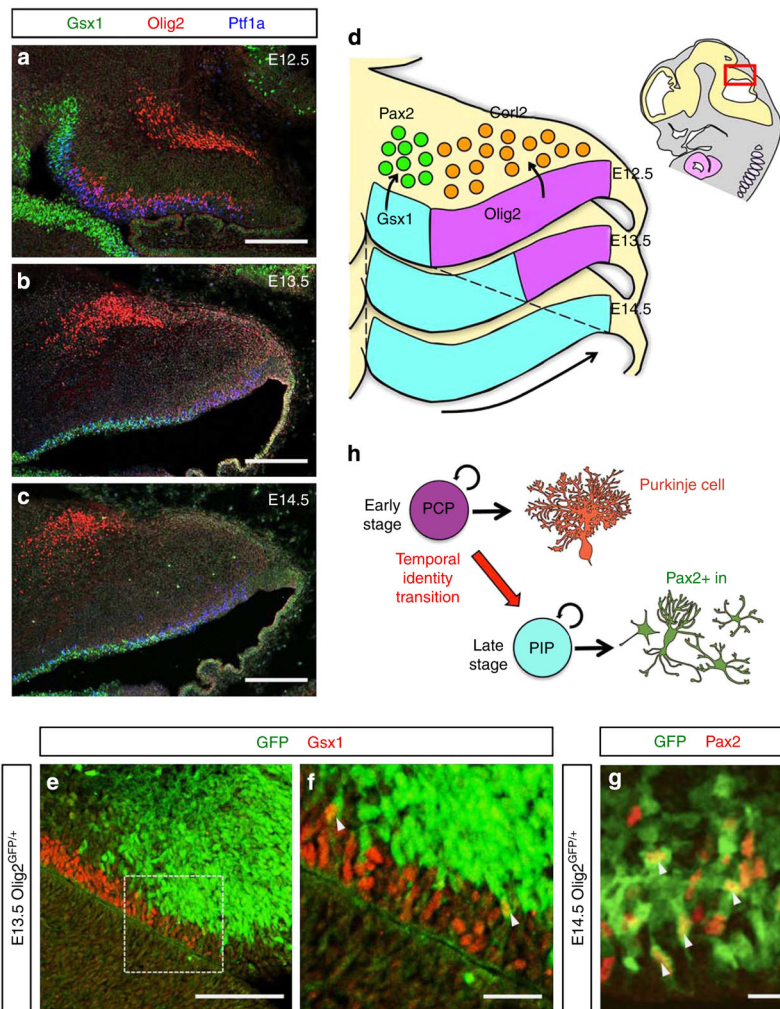


Figure 3. Temporal identity transition of cerebellar GABAergic neuron progenitors
(a–d) Developmental changes of localization of PCPs and PIPs in the embryonic cerebellar VZ. **(a–c)** Immunostaining with Gsx1, Olig2 and Ptf1a in **(a)** E12.5, **(b)** E13.5 and **(c)** E14.5 cerebella. **(d)** Schematic diagram of developmental changes of Gsx1- and Olig2-expressing regions in the cerebellar VZ. As development proceeds, Gsx1-expressing region expands to the dorsal region, while Olig2-expressing region shrinks. **(e–g)** Intermediate-term lineage trace using *Olig2^{GFP/+}* embryos to investigate the lineage relationship between PCPs and PIPs. Cerebellar primordium of *Olig2^{GFP/+}* at E13.5 **(e,f)** or E14.5 **(g)** was immunostained with indicated antibodies. Arrowheads highlight double-positive cells for GFP and the marker. **(f)** High magnification of the rectangle in **(e)**. **(h)** Schematic diagram of temporal identity transition of cerebellar GABAergic neuron progenitors from PCPs to PIPs. PCPs at early stages change their character to become PIPs at late embryonic stages and start to generate Pax2 + INs. Scale bars represent: **(a–c,e)** 100 μ m, **(f)** 25 μ m, **(g)** 10 μ m.

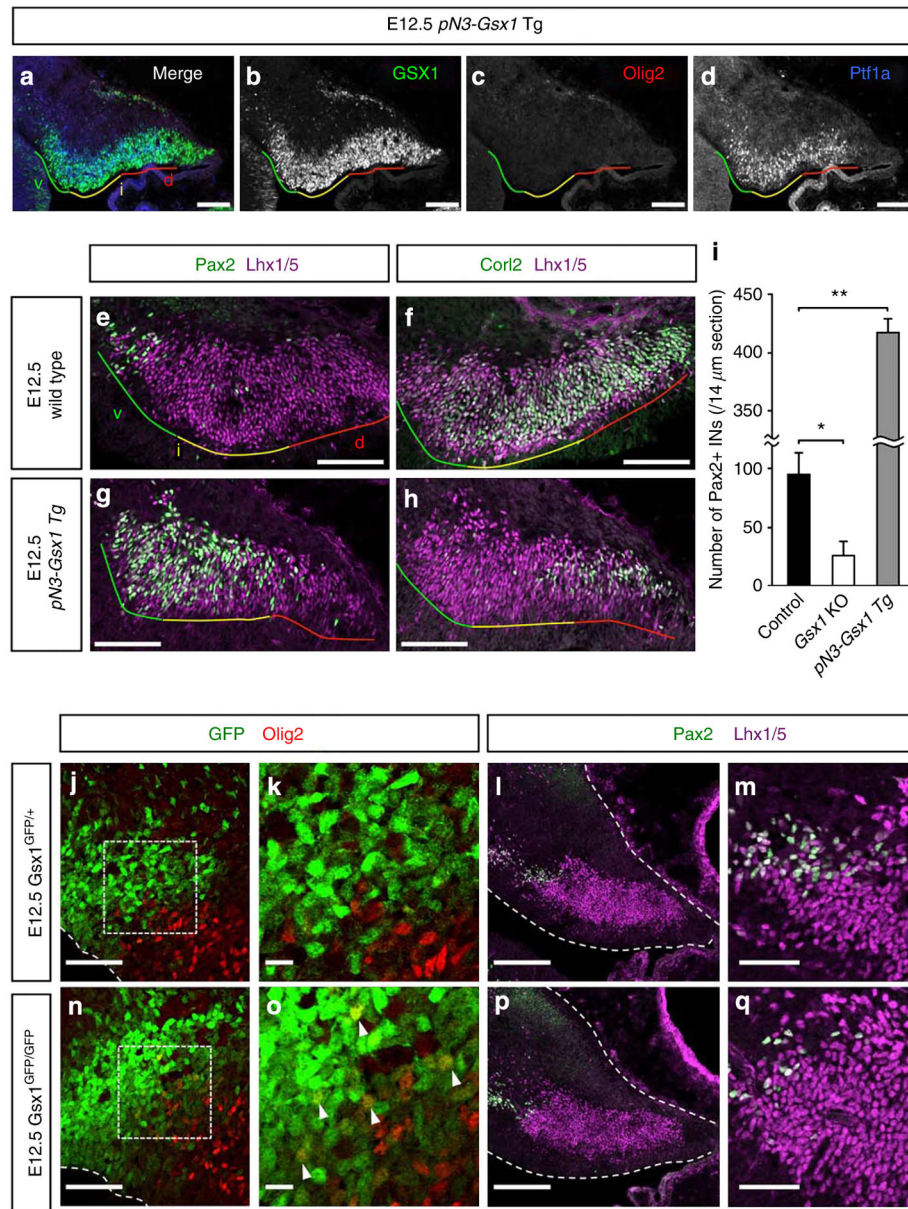


Figure 4. Phenotypes of *pN3-Gsx1* Tg and *Gsx1* KO mice

(a–d) Cerebellar primordium of E12.5 *pN3-Gsx1* Tg mouse stained with antibodies for Gsx1, Ptf1a and Olig2. Coloured lines indicate ventral (green), intermediate (yellow) and dorsal (red) regions of cerebellar VZ, respectively. (e–h) Cerebellar primordium of E12.5 (e,f) wild-type or (g,h) *pN3-Gsx1* Tg mouse stained with antibodies for (e,g) Pax2 or (f,h) Corl2 and Lhx1/5. Postmitotic GABAergic neurons are labelled with an antibody for Lhx1/5 at this stage. (i) The average number of Pax2 + INs per slice of control (wild type and *Gsx1*^{GFP/+}), *Gsx1*^{GFP/GFP} and *pN3-Gsx1* Tg embryos ($n = 3$, * $P < 0.05$, ** $P < 0.01$ by t -test, mean \pm s.e.m.). (j–q) Immunostaining of E12.5 *Gsx1*^{GFP/+} (j–m) and *Gsx1*^{GFP/GFP} (n–q) cerebella with indicated antibodies. Scale bars represent (a–h,l,p) 100 μ m, (j,m,n,q) 50 μ m, (k,o) 10 μ m.

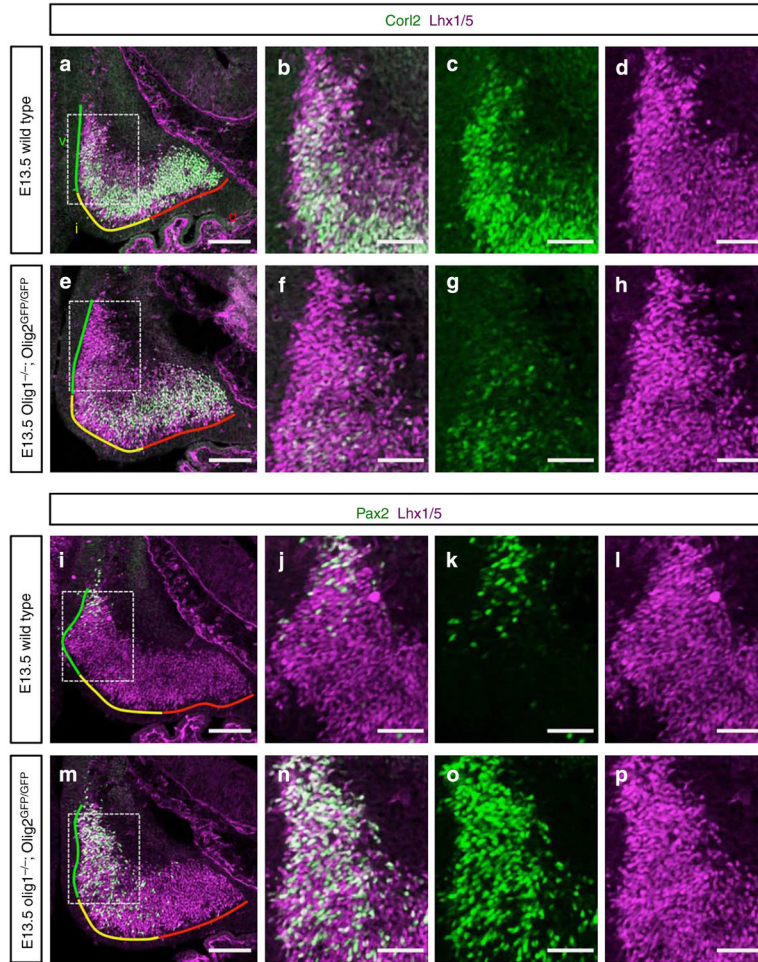


Figure 5. Phenotypes of *Olig1/2* dKO mice

(a,e) Cerebellar primordium of E13.5 (a) wild-type and (e) *Olig1/2* dKO mouse stained with antibodies for Corl2 and Lhx1/5. Coloured lines indicate ventral (green), intermediate (yellow) and dorsal (red) regions of cerebellar primordia, respectively. (b–d,f–h) Higher-magnification images of the rectangular regions in (a) and (e), respectively. (i,m) Cerebellar primordium of E13.5 (i) wild-type and (m) *Olig1/2* dKO mouse stained with antibodies for Pax2 and Lhx1/5. (j–l,n–p) Higher-magnification images of the rectangular regions in (i) and (m), respectively. Scale bars represent (a,e,i and m) 100 μ m, (b–d,f–h,j–l and n–p) 50 μ m.

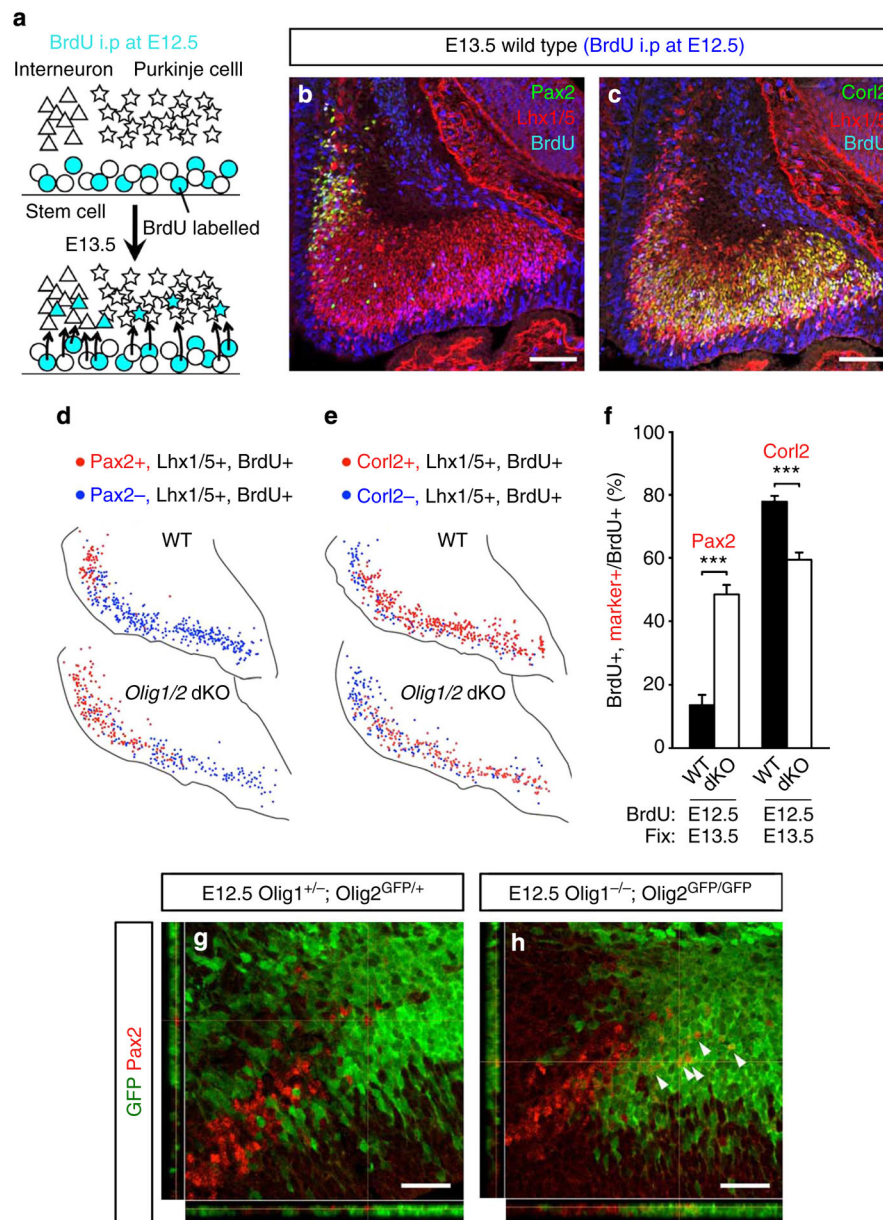


Figure 6. Altered fates of GABAergic neurons generated around E12.5 in *Olig1/2* dKO mice
(a) Schematic diagram of BrdU incorporation experiment. At E12.5, intraperitoneal injection of BrdU was performed and cells in S-phase (progenitors) incorporated BrdU. At E13.5 postmitotic neurons generated from BrdU-labelled progenitors can also be labelled with BrdU. The number and the position of BrdU-labelled GABAergic interneurons and Purkinje cells predicts a general distribution of PIPs and PCPs at E12.5, respectively. **(b,c)** Examples of immunostaining of E13.5 wild-type cerebellum using antibodies for BrdU, Lhx1/5 and **(b)** Pax2 or **(c)** Corl2. Immunostaining of Lhx1/5 enables the distinction of BrdU-labelled postmitotic neurons from BrdU-labelled mitotic progenitors. **(d,e)** Representative images of plots of indicated cells in wild-type and *Olig1/2* dKO cerebella. **(f)** The ratio of BrdU-labelled Pax2 + INs or Purkinje cells to BrdU-labelled GABAergic

neurons in wild-type and *Olig1/2* dKO cerebella ($n=3$, *** $P<0.001$ by t -test, mean \pm s.e.m.). **(g,h)** Short-term lineage tracing analyses using **(g)** heterozygotes and **(h)** homozygotes of *Olig1/2* dKO line. Arrowheads indicate GFP-positive Pax2 INs. Scale bars represent **(b,c)** 100 μ m, **(g,h)** 25 μ m.

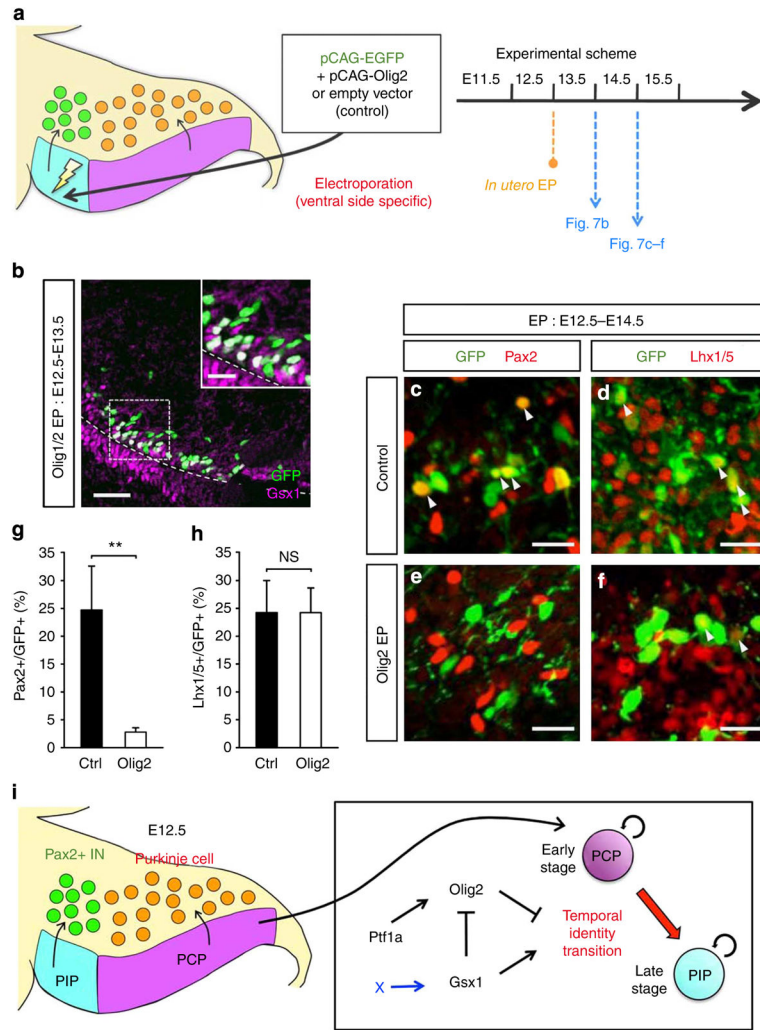


Figure 7. Ectopic expression of Olig2 in Gsx1-expressing progenitors

(a) Schematic diagram of *in utero* electroporation. Plasmid DNA was injected into the fourth ventricle and electroporated to the Gsx1-expression region at E12.5. The electroporated brains were collected at E13.5 or E14.5. (b) Immunostaining of E13.5 wild-type cerebellum electroporated with Olig2 at E12.5. Antibodies are indicated. (c–f) Sections of E14.5 wild-type mice electroporated with (c,d) control and (e,f) Olig2. Regions just above the Gsx1-expressing cells are shown. Arrowheads indicate co-immunostaining of GFP and the marker. (g,h) Quantification of the percentages of (g) Pax2-positive cells and (h) Lhx1/5-positive cells in electroporated cells ($n=3$, NS, not significant, $**P<0.01$ by t -test, $\text{mean}\pm\text{s.e.m.}$). (i) Summary of this study. Scale bars represent (b) 25 μm , (inset of b,c–f) 10 μm .